varied[11], but also as the magnetic field is imposed for fixed x (ref. 17). The anisotropic field effect reflects the anisotropy of other physical properties, such as the magnetic penetration depth and coherence length. Thus, the persistence of the effect above T_c would naturally be due to superconducting fluctuations or incoherent pairing, which also display this anisotropy in the normal state. Such fluctuations exist in models postulating a Bose–Einstein condensation of pre-formed pairs at T_c in the underdoped copper oxides[12–14]. □

1. Anderson, P. W. The resonating valence bond state in La$_2$CuO$_4$. *Science* **235,** 1196–1198 (1987).
2. Emery, V. J. Theory of high-T_c superconductivity in oxides. *Phys. Rev. Lett.* **58,** 2794–2797 (1987).
3. Hirsch, J. E. Antiferromagnetism, localization, and pairing in a two-dimensional model for CuO$_2$. *Phys. Rev. Lett.* **59,** 228–231 (1987).
4. Schulz, H. J. Superconductivity and antiferromagnetism in the two-dimensional Hubbard model: scaling theory. *Europhys. Lett.* **4,** 609–615 (1987).
5. Scalapino, D. J. The cuprate pairing mechanism. *Science* **284,** 1282–1283 (1999).
6. Rossat-Mignod, J. et al. Neutron scattering study of the YBa$_2$Cu$_3$O$_{6+x}$ system. *Physica C* **185–189,** 86–92 (1991).
7. Mook, H. A., Yethiraj, M., Aeppli, G., Mason, T. E. & Armstrong, T. Polarized neutron determination of the magnetic excitations in YBa$_2$Cu$_3$O$_7$. *Phys. Rev. Lett.* **70,** 3490–3493 (1993).
8. Fong, H. F. et al. Phonon and magnetic neutron scattering at 41 meV in YBa$_2$Cu$_3$O$_7$. *Phys. Rev. Lett.* **75,** 316–319 (1995).
9. Dai, P., Yethiraj, M., Mook, H. A., Lindemer, T. B. & Doğan, F. Magnetic dynamics in underdoped YBa$_2$Cu$_3$O$_{7-x}$: direct observations of a superconducting gap. *Phys. Rev. Lett.* **77,** 5425–5428 (1996).
10. Fong, H. F., Keimer, B., Milius, D. L. & Aksay, I. A. Superconducting-induced anomalies in the spin excitation spectra of underdoped YBa$_2$Cu$_3$O$_{6+x}$. *Phys. Rev. Lett.* **78,** 713–716 (1997).
11. Dai, P. et al. The magnetic excitation spectrum and thermodynamics of high-T_c superconductors. *Science* **284,** 1344–1347 (1999).
12. Uemura, Y. J. Bose-Einstein to BCS crossover picture for high-T_c cuprates. *Physica C* **282,** 194–197 (1997).
13. Emery, V. J. & Kivelson, S. A. Importance of phase fluctuations in superconductors with small superfluid density. *Nature* **374,** 434–437 (1995).
14. Lee, P. A. & Wen, X. G. Unusual superconducting state of underdoped cuprates. *Phys. Rev. Lett.* **78,** 4111–4114 (1997).
15. Junod, A., Erb, A. & Renner, Ch. Specific heat of high temperature superconductors in high fields at T_c: from BCS to the Bose-Einstein condensation. *Physica C* **317,** 333–344 (1999).
16. Junod, A. in *Studies of High Temperature Superconductors* Vol. 19 (ed. Narlikar, A. V.) 1 (Nova Science, New York, 1996).
17. Janko, B. Thermodynamic constraints on the magnetic field dependence of the neutron resonance in cuprate superconductors. Preprint cond-mat/9912073 at ⟨http://xxx.lanl.gov⟩ (1999; cited 6 Dec. 1999).
18. Tranquada, J. M. et al. Neutron-diffraction determination of antiferromagnetic structure of Cu ions in YBa$_2$Cu$_3$O$_{6+x}$ with $x = 0.0$ and 0.15. *Phys. Rev. Lett.* **60,** 156–159 (1988).
19. Bourges, P. et al. High magnetic field dependence of spin fluctuations in YBa$_2$Cu$_3$O$_7$. *Physica B* **234–236,** 830–831 (1997).
20. Dai, P., Mook, H. A. & Doğan, F. Incommensurate magnetic fluctuations in YBa$_2$Cu$_3$O$_{6.6}$. *Phys. Rev. Lett.* **80,** 1738—1741 (1998).
21. Mook, H. A. et al. Spin fluctuations in YBa$_2$Cu$_3$O$_{6.6}$. *Nature* **395,** 580–582 (1998).
22. Hayden, S. M. et al. Absolute measurements of the high-frequency magnetic dynamics in high-T_c superconductors. *Physica B* **241–243,** 765–772 (1998).
23. Aeppli, G. et al. The weights of various features in the magnetic spectra of cuprates. *Phys. Status Solidi B* **215,** 519–522 (1999).
24. Arovas, D. P., Berlinsky, A. J., Kallin, C. & Zhang, S. C. Superconducting vortex with antiferromagnetic core. *Phys. Rev. Lett.* **79,** 2871–2874 (1997).
25. Anderson, P. W. Two crucial experimental tests of the resonating valence bond-Luttinger liquid interlayer tunneling theory of high-T_c superconductivity. *Phys. Rev. B* **42,** 2624–2626 (1990).
26. Renner, Ch., Revaz, B., Genoud, J.-Y., Kadowaki, K. & Fischer, Ø. Pseudogap precursor of the superconducting gap in under- and overdoped Bi$_2$Sr$_2$CaCu$_2$O$_{8+\delta}$. *Phys. Rev. Lett.* **80,** 149–152 (1998).
27. Basov, D. N. et al. Sum rules and interlayer conductivity of high-T_c cuprates. *Science* **283,** 49–52 (1999).
28. Yin, L., Chakravarty, S. & Anderson, P. W. The neutron peak in the interlayer tunneling model of high temperature superconductors. *Phys. Rev. Lett.* **78,** 3559–3562 (1997).
29. Scalapino, D. J. & White, S. R. Superconducting condensation energy and an antiferromagnetic exchange-based pairing mechanism. *Phys. Rev. B* **58,** 8222–8224 (1998).
30. Demler, E. & Zhang, S. C. Quantitative test of a microscopic mechanism of high-temperature superconductivity. *Nature* **396,** 733–735 (1998).
31. Chakravarty, S. & Kee, H.Y. Measuring condensate fraction in superconductors. *Phys. Rev. B* **61,** 14821–14824 (2000).

Quantum correlation among photons from a single quantum dot at room temperature

P. Michler*, A. Imamoğlu*, M. D. Mason†, P. J. Carson†, G. F. Strouse† & S. K. Buratto†

* *Department of Electrical and Computer Engineering, and Department of Physics, University of California, Santa Barbara, California 93106, USA*
† *Department of Chemistry and Biochemistry, University of California, Santa Barbara, California 93106, USA*

....

Maxwell's equations successfully describe the statistical properties[1,2] of fluorescence from an ensemble of atoms or semiconductors in one or more dimensions. But quantization of the radiation field is required to explain the correlations of light generated by a single two-level quantum emitter, such as an atom, ion or single molecule[3–6]. The observation of photon antibunching in resonance fluorescence from a single atom unequivocally demonstrated the non-classical nature of radiation[3]. Here we report the experimental observation of photon antibunching from an artificial system—a single cadmium selenide quantum dot at room temperature. Apart from providing direct evidence for a solid-state non-classical light source, this result proves that a single quantum dot acts like an artificial atom, with a discrete anharmonic spectrum. In contrast, we find the photon-emission events from a cluster of several dots to be uncorrelated.

The physics of photon antibunching is easy to understand: if a two-level atom emits a photon at time $\tau = 0$, it is impossible for it to emit another one immediately after, because it is necessarily in the ground state. The next photon can only be emitted after a waiting time, which, under weak excitation conditions, is determined by the spontaneous emission time. The result is that there is a dead-time between successive photon-emission events, and the generated photon stream, in the absence of other sources of fluctuation, is sub-poissonian[1]. Photon antibunching is easily washed away with increasing number of atoms. Conversely, we can consider strong photon antibunching as evidence that the source of the radiation field is a single anharmonic (for example, two-level) quantum system: if the spectrum of the emitter is harmonic or there is more than one anharmonic emitter, then the detection of the first
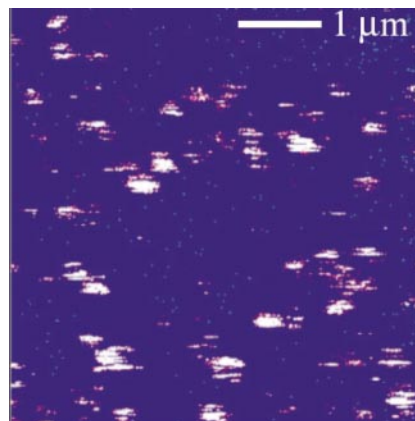

Figure 1 Photoluminescence image of CdSe/ZnS nanocrystals on a glass plate. Image was acquired by raster scanning the particle-covered glass plate through the laser focus ($\lambda = 488$ nm, FWHM was 300 nm) and collecting the photoluminescence onto a single-photon-counting avalanche photodiode. This 256×256 pixel image (4.9 ms per pixel) represents an $5 \times 5\ \mu m^2$ field of view.

photon at $\tau = 0$ will no longer guarantee that the whole system is in its (radiatively inactive) ground state immediately after $\tau = 0$.

Photon correlation measurements on single quantum dots (QDs) were carried out by combining a Hanbury–Brown–Twiss photon coincidence set-up with a confocal scanning optical microscope (CSOM). All measurements were carried out at room temperature. To the best of our knowledge, this is the first QD experiment that goes beyond first-order optical coherence measurements[1].

Figure 1 shows a typical confocal image ($5 \times 5\,\mu m$) of CdSe/ZnS nanoparticles on a glass plate. Each bright spot corresponds to the luminescence from either a single CdSe/ZnS quantum dot or a cluster of several dots. However, it is important to note that the smallest spot size ($\sim 300\,nm$) is defined by the resolution of the CSOM. As can be seen, bright spots with different sizes are visible and the smallest spots appear to blink 'on' and 'off' during the course of a scan[7]. This behaviour is thought to be the result of QD ionization, which will be discussed in more detail below.

The measured raw data photon correlation signals from a cluster of several QDs and a single CdSe/ZnS quantum dot are shown in Fig. 2. The single QD data shows a minimum of coincidence counts $n(\tau)$ around a pair separation time of $\tau = 0$, and an exponential increase of $n(\tau)$ for negative and positive values of τ. This is a clear signature of non-classical photon antibunching[1,3]. In contrast, the photon correlation signal of the CdSe/ZnS cluster is flat. In this case many independently radiating QDs contribute to the signal.

Quantum dots are fairly complicated artificial atoms. Even for an isolated QD, the optical transitions have non-trivial signatures such as spectral diffusion and relatively large non-radiative broadening[8]. To model our photon correlation experiment, we use a simple three-state model for the QDs. We assume that the excited electron–hole pair relaxes incoherently before spontaneously emitting a photon: this relaxation process between the two excited states is much faster than other relevant rates[9]. In addition, we have introduced a fast, elastic dephasing rate for the coherences between the ground and excited states. Using the quantum regression theorem, we derive an expression for the normalized second-order correlation function[1] $g^{(2)}(\tau) = \langle : I(t)I(t+\tau) : \rangle / \langle I(t) \rangle^2$ (where : : indicates normal ordering and $I(t)$ is the measured intensity) in the weak-laser excitation regime

$$g^{(2)}(\tau) = 1 - e^{-(\Gamma + W_p)\tau}. \qquad (1)$$

Here Γ is the electron–hole recombination rate and W_p is the effective pump rate into the radiatively active upper state. The fast dephasing of the emitting transition has no effect on $g^{(2)}(\tau)$ of a single QD. In contrast, for an ensemble of dots, the bosonic bunching effect decays with the dephasing time, which is estimated to be at least 10 ps using the narrowest observed linewidths[8]. This result indicates that with the time resolution of our experiment $\tau_{res} = 420\,ps$, we should expect to find uncorrelated photon counting events for an ensemble of dots (that is, $g^{(2)}(\tau) = 1$). The
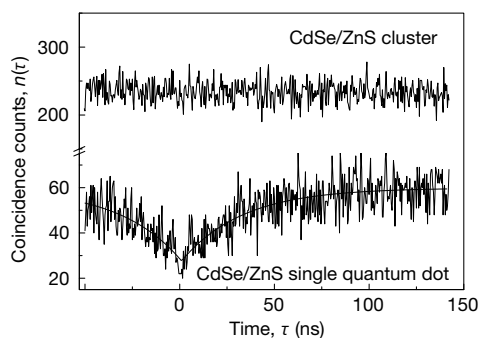
experimental observations discussed earlier are fully consistent with this prediction. We remark that the measured $n(\tau)$ follows the autocorrelation $g^{(2)}(\tau)$ in the limit where the reciprocal of the average counting rate is much longer than the monitored time range. As this is always the case for our measurements, we calculate $g^{(2)}(\tau)$ by normalizing $n(\tau)$ to the long time average of 60 counts per channel.

The single QD data are fitted by $g^{(2)}(\tau) = 1 - ae^{-\tau/t_d}$ with decay time $t_d = 1/(\Gamma + W_p)$ and a being fit parameters. The factor a is introduced to take care of the stray-light background and residual biexcitonic effects. We obtain $t_d = 32 \pm 2\,ns$ which directly determines the single electron–hole pair lifetime under our experimental conditions ($\Gamma \gg W_p$). This value is of the same order of magnitude as independent lifetime measurements on ensembles of QDs. The fit also gives an estimate of $g^{(2)}(0) = 0.47 \pm 0.02$, which is a clear signature of non-classical photon antibunching from a single anharmonic quantum system.

The QD photoluminescence intensity versus time was recorded with an integration time of 2 ms per bin and typical scan durations of 5 to 30 min. Figure 3a and b shows the photoluminescence intensity time trace of a single CdSe/ZnS quantum dot in the long time range. An irregular and multi-level intensity emission is observed for the chosen size of the time bins. The background level of 3,000 counts s⁻¹ is visible around 151 s in Fig. 3b where the CdSe quantum dot is in an 'off' state. This turning 'on' and 'off' behaviour (blinking) has been interpreted in terms of an Auger ionization model[7,10]. In the case where two electron–hole pairs are excited in the QD, the recombination energy (~ 2.14 eV) of the first pair can be used to eject either the electron or the hole from the second pair into a deep trap of the surrounding matrix. A CdSe quantum dot ionized in this way is predominantly non-emissive, that is, in an 'off' state[7]. The bright state, that is, the 'on' state, is recreated either by recapturing the ejected carrier or through a second Auger process. The fast Auger rate is therefore not only responsible for the blinking of the QDs but also reduces the exciton-to-biexciton transition amplitude, making the virtual amplitude in the biexciton state small. However, one would still expect to find $g^{(2)}(0) > 0$ due to residual biexciton luminescence.

Figure 4 shows the calculated classical intensity autocorrelation function $G^{(2)}(\tau) = \langle I(t)I(t+\tau) \rangle / \langle I(t) \rangle^2$ for the time trace of Fig. 3. The signature of blinking at this timescale is the bunching behaviour ($G^{(2)}(0) > 1$). Clearly, the photon-bunching due to QD blinking can be described classically and has to be distinguished from the photon antibunching observed in the short time range (0–200 ns), which is due to the quantum nature of the emitter. The fact that the photon pair distribution remains flat for $100\,ns \leqslant \tau \leqslant 150\,ns$ is a good

Figure 2 Measured distribution $n(\tau)$ of photon pair separation times τ for a CdSe/ZnS cluster and a single quantum dot. The line represents a fit to an exponential law and is described in the text.
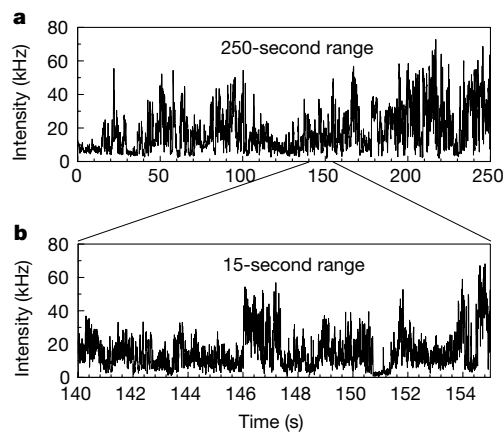
Figure 3 Time trace of photoluminescence intensity of a single CdSe/ZnS quantum dot on two different timescales. **a**, 250-second time range with 62.5 ms per bin. **b**, Expanded time range (15 seconds) with 3.9 ms per bin.
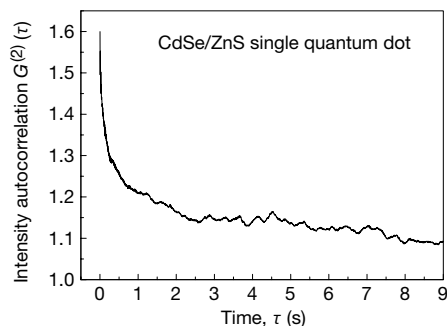
Figure 4 Intensity autocorrelation $G^{(2)}(\tau)$ obtained for the time trace shown in Fig. 3.

indication that blinking does not occur on the timescales of interest for photon antibunching.

Prior measurements on single QD photoluminescence and absorption have demonstrated the existence of discrete QD resonances[8]. However, just as the observation of discrete absorption lines in an atomic vapour cannot be taken as an evidence that the observed system consists of a single atom, these experiments, at least in principle, cannot rule out the existence of several QDs. In contrast, photon correlation measurements, such as the one reported here, provide a reliable method for deciding whether or not the observed system is a single anharmonic quantum emitter. In addition, owing to interactions with the lattice, a nanostructure that acts like an anharmonic emitter at cryogenic temperatures can be indistinguishable from a higher-dimensional system at room temperature. We have demonstrated that a CdSe quantum dot behaves as an anharmonic emitter even at room temperature. Our results constitute a first step in the study of quantum optical phenomena in semiconductor QDs. Demonstration of quantum dynamics in semiconductors at room temperature could lead to applications in quantum information processing and computation. □

Methods

Sample preparation

The CdSe/ZnS (core/shell) quantum dots were synthesized following high-temperature organometallic methods described in the literature[11–13]. The resulting nanoparticles were capped with the organic ligand trioctylphosphine oxide (TOPO) and had a distribution with an average diameter of 4.1 nm and a r.m.s. (root mean square) width of 0.33 nm (8% size distribution). The single QD samples were prepared by spin-casting 30 μl of a 0.5 nM solution of the QDs dissolved in hexanes onto a bare glass coverslip, which resulted in a mean separation of the QDs of approximately 1 μm.

Experimental set-up

Optical pumping was performed using circularly polarized light of the 488-nm line of a continuous-wave Ar$^+$ laser, generating electron–hole pairs in the excited states of the CdSe quantum dots. The exciting light was focused by a high numerical aperture (NA = 1.3) oil-immersion objective to a near-diffraction-limited (full-width at half-maximum (FWHM)) spot approximately 300 nm in diameter at the glass–sample interface. In order to minimize the generation of two electron–hole pairs simultaneously we used a low excitation intensity of about 250 W cm^{-2}. Typically, a QD was excited approximately every 1–10 μs (ref. 14), whereas the photoluminescence decay time is of the order of 30 ns. Thus the probability of generating two electron–hole pairs was small. The photoluminescence from the QD was collected by the same objective and first passed through the excitation laser beam splitter and then through a holographic notch filter to block scattered laser light. The light was then split with a 50/50 non-polarizing beam splitter and the resulting two photon beams were focused onto the active areas of two single-photon-counting avalanche photodiodes (SPAD).

Measurement

Photoluminescence images of the nanocrystals were obtained by scanning the QD-covered glass plate through the laser focus and recording the number of counts with one of the SPADs. To measure the photon statistics of a selected QD (or a cluster of QDs), the glass plate was positioned where a single bright spot of typically 300 nm in diameter (resolution limited) was observed in the photoluminescence image. The number of pairs of photons $n(\tau)$ with arrival-time separations of τ was measured using the two SPADs for $\tau \leqslant \tau_{max} = 200$ ns. The pulses from the two SPADs were used to start and stop a time-to-amplitude converter (TAC) where the time delay between the start and stop pulses (to within τ_{res}) was converted to a voltage amplitude. The SPADs exhibited the same counting

rate. An electronic delay (53 ns) was introduced in the stop channel in order to check the symmetry of the $n(\tau)$ signal and to avoid the effect of noise for small voltages in the TAC. The output pulses were fed into a multichannel analyser. To reduce the background contribution and therefore decrease the amount of uncorrelated light in the $n(\tau)$ measurement, the multichannel analyser was enabled only during the 'on' periods, that is, when the signal level was above a certain threshold.

1. Walls, D. F. & Milburn, G. J. *Quantum Optics* (Springer, Berlin, 1994).
2. Hanbury-Brown, R. & Twiss, R. Q. Correlation between photons in two coherent beams of light. *Nature* **177,** 27–29 (1956).
3. Kimble, H. J., Dagenais, M. & Mandel, L. Photon antibunching in resonance fluorescence. *Phys. Rev. Lett.* **39,** 691–694 (1977).
4. Diedrich, F. & Walther, H. Nonclassical radiation of a single stored ion. *Phys. Rev. Lett.* **58,** 203–206 (1987).
5. Basché, Th., Moerner, W. E., Orrit, M. & Talon, H. Photon antibunching in the fluorescence of a single dye molecule trapped in a solid. *Phys. Rev. Lett.* **69,** 1516–1519 (1992).
6. Fleury, L., Segura, J.-M., Zumofen, G., Hecht, B., Wild, U. P. Nonclassical photon statistics in single-molecule fluorescence at room temperature. *Phys. Rev. Lett.* **84,** 1148–1151 (2000).
7. Nirmal, M. *et al.* Fluorescence intermittency in single cadmium selenide nanocrystals. *Nature* **383,** 802–804 (1996).
8. Empedocles, S. & Bawendi, M. G. Spectroscopy of single CdSe nanocrystallites. *Acc. Chem. Res.* **32,** 389–396 (1999).
9. Klimov, V. I. & McBranch, D. W. Femtosecond 1P-to-1S electron relaxation in strongly confined semiconductor nanocrystals. *Phys. Rev. Lett.* **98,** 4028–4031 (1998).
10. Efros, Al. L. & Rosen, M. Random telegraph signal in the photoluminescence intensity of a single quantum dot. *Phys. Rev. Lett.* **78,** 1110–1113 (1997).
11. Murray, C. B., Norris, D. J. & Bawendi, M. G. Synthesis and characterization of nearly monodisperse CdE (E = S, Se, Te) semiconductor nanocrystallites. *J. Am. Chem. Soc.* **115,** 8706–8715 (1993).
12. Hines, M. A. & Guyot-Sionnest, P. Synthesis and characterization of strongly luminescing ZnS-capped CdSe nanocrystals. *J. Phys. Chem.* **100,** 468–571 (1996).
13. Dabbousi, B. O. *et al.* (CdSe)ZuS core shell quantum dots: synthesis and characterization of a size series of highly luminescent nanocrystallites. *J. Phys. Chem.* **101,** 9463–9475 (1997).
14. Nirmal, M. & Brus, L. Luminescence photophysics in semiconductor nanocrystals. *Acc. Chem. Res.* **32,** 407–414 (1999).

....

Organoplatinum crystals for gas-triggered switches

Martin Albrecht*, **Martin Lutz**†, **Anthony L. Spek**† & **Gerard van Koten***‡

* *Debye Institute, Department of Metal-Mediated Synthesis &* † *Bijvoet Center for Biomolecular Research, Crystal and Structural Chemistry, Utrecht University, Padualaan 8, 3584 CH Utrecht, The Netherlands*

....

Considerable effort is being devoted to the fabrication of nano-scale devices[1]. Molecular machines, motors and switches have been made, generally operating in solution[2–7], but for most device applications (such as electronics and opto-electronics), a maximal degree of order and regularity is required[8]. Crystalline materials would be excellent systems for these purposes, as crystals comprise a vast number of self-assembled molecules, with a perfectly ordered three-dimensional structure[9]. In non-porous crystals, however, the molecules are densely packed and any change in them (due, for example, to a reaction) is likely to destroy the crystal and its properties. Here we report the controlled and fully reversible crystalline-state reaction of gaseous SO$_2$ with non-porous crystalline materials consisting of organoplatinum molecules. This process, including repetitive expansion–reduction sequences (on gas uptake and release) of the crystal lattice, modifies the structures of these molecules without affecting their crystallinity. The process is based on the incorporation of SO$_2$ into the colourless crystals and its subsequent liberation from